Immunohistochemical and ultrastructural study of the lamellae of oocytes in atretic follicles in relation to different processes of cell death

M.L. Escobar, O.M. Echeverría, G. García, R. Ortiz, G.H. Vázquez-Nin

Laboratorio de Microscopía Electrónica, Departamento de Biología Celular, Facultad de Ciencias, Universidad Nacional Autónoma de México, Coyoacán, Mexico

Abstract

Atresia is the process through which non-selectable oocytes are eliminated; it involves apoptosis and/or autophagy. This study used immunohistochemical and ultrastructural techniques to characterize the lamellae present in the cytoplasm of oocytes in follicles in the process of atresia in prepubertal and adult Wistar rats. The results indicate that the lamellae are positive to tubulin and myosin immunodetection under light and electron microscopy. Labeling is greater with anti-tubulin and lesser with anti-myosin. Our observations indicate that lamellae are present in oocytes at the initial antral stage in prepubertal rats; that is, from day 14 post-birth to adult age. We were able to determine that the increase in altered lamellae principally occurs in the apoptotic cells rather than in the autophagic cells.

Introduction

Mammalian ovaries consist of follicles that undergo several maturation processes before developing the features of one, or several, selectable follicles with a fertilizable oocyte. The oocytes that will not be ovulated are degraded *via* a process called follicular atresia. In previous reports, two types of cell death were described during follicular atresia in Wistar rats: apoptosis and autophagy.[1-5] Type 1 programmed cell death, known as apoptosis, is morphologically characterized by cell shrinkage, nuclear condensation, membrane blebbing, and the formation of apoptotic bodies.[6] Biochemically, it is characterized by the presence of the active form of proteases called caspases, which exist in an inactive form in the cytoplasm. Once activated, the caspases are responsible for the morphological characteristics of apoptosis.[7] Apoptosis is activated by two different pathways, called extrinsic and intrinsic. The extrinsic pathway is triggered by membrane receptors that induce cleavage and activation of the pro-caspase-8 initiator.[8] Once caspase-8 is activated it can, in turn, activate the executer caspases -3, -6 and -7,[7] which then exert their effect on several target proteins, including components of the cytoskeleton.[9,10]

Autophagic cell death, also called type II programmed cell death, includes various morphological characteristics, comprising an increased number of autophagic vesicles with cytoplasmic content in different degrees of degradation. Autophagy begins with the formation of double membrane-bound cytoplasmic vacuoles that surround cytoplasmic macromolecules and organelles.[11] The molecular characteristics of autophagy entail activation of *Atg* (autophagy-related genes),[12] along with the autophagic pathway. The autophagic process is associated with the dynamics of the cytoskeleton; in fact, the microtubule-associated protein 1A/1B-light chain 3 (LC3/Atg8) has been correlated with regulation of the assembly and disassembly of microtubules. Today we know that LC3 plays an important role in the formation of autophagosomes and is present in the cytosol in the form LC3-I. During autophagy, it is lipidated to produce the complex LC3-phosphatidylethanolamine, known as form LC3-II, which is recruited to the membrane of the autophagosome.[13] The LC3 protein has been considered essential for the study of the autophagy process. Vázquez-Nin and Sotelo[14] evidenced ultrastructural changes in the oocyte during the process of elimination, including the presence of lamellae with different arrangements. Considering that both apoptotic and autophagic features are present during oocyte cell death, it is important to achieve a better understanding of the behavior of the lamellae and their modifications during the processes of cell death, and of their relationships with the components of the cytoskeleton.

The aim of the present study, therefore, is to examine the different distribution patterns of lamellae during the process of atresia in the oocytes of prepubertal and adult rats, and their correlation with components of the cytoskeleton by means of immunohistochemical and ultrastructural analyses. We found that microtubule depolymerization increases greatly in the oocytes of antral follicles that were positive to the pro-apoptotic markers. In contrast, the oocytes that were positive to markers of autophagy presented less depolymerization of the components of the cytoskeleton. These results indicate that the lamellae identified at the ultrastructural level correspond to cytoskeleton compounds that increase more in apoptotic than autophagic cell death.

Correspondence: Dr. Gerardo Hebert Vázquez-Nin, Universidad Nacional Autónoma de México, Ciudad Universitaria, Delegación Coyoacán C.P. 04510, México.
Tel. +521.55.56224881 - Fax: +521.55.56224828.
E-mail: vazqueznin@ciencias.unam.mx

Keywords: Atresia; apoptosis; autophagy; cytoskeleton; tubulin.

Contributions: EML, EOM, VNGH, experiments design, research performing, manuscript writing; GG, Western Blot assays; OR, histologic interpretation.

Conflict of interest: the authors declare no conflict of interest.

Acknowledgments: this work was supported by the grant CONACyT 180526. The authors would like to thank Ernestina Ubaldo Pérez for technical assistance. They also thank Paul C. Kersey Johnson for reviewing the English word usage and grammar.

Received for publication: 7 May 2015.
Accepted for publication: 24 June 2015.

European Journal of Histochemistry 2015; 59:2535
doi:10.4081/ejh.2015.2535

Materials and Methods

The animals were handled in accordance with the ethical guidelines recommended in the Guidelines for the Care and Use of Laboratory Animals.[15] Ovaries from 33 prepubertal (1-28 day-old) and adult 30 Wistar rats were used for analysis under light and electron microscopy and Western Blot assays.

Ovary embedding

Paraffin embedding: ovaries were fixed by immersion in 2% paraformaldehyde in phosphate-buffered saline (PBS) at pH 7.2 for 2 h at room temperature, embedded in paraffin, and sectioned (10 µm). The sections from each ovary were aligned on glass microscope slides covered with poly-l-lysine (Sigma, Toluca, Mexico). Observations were made under a Nikon Eclipse E600 microscope.

Lowicryl K4M embedding: ovaries were fixed by immersion in 4% paraformaldehyde in phosphate-buffered saline (PBS) at pH 7.2 for 2 h at room temperature and embedded in Lowicryl K4M plastic resin. They were then sectioned at different thicknesses: 700 nm and 60 nm for light and electron immunodetection, respectively. The 700-nm-thick sections were aligned on glass slides covered with poly-l-lysine, while the 60-nm sections were aligned in single slot grids (Electron Microscopy Sciences, Hatfield, PA, USA). The semi-thin sections (700 nm) were evaluated under a Nikon Eclipse E600 microscope, while the ultra-thin sections (60 nm) were examined under a JEOL 1010 electron microscope operated at 100 KV. Epon embedding: ovaries were fixed by immersion in 2.5% glutaraldehyde-4% paraformaldehyde in phosphate-buffered saline (PBS) at pH 7.2 for 2 h. After rinsing in the same buffer, tissues were post-fixed in 1% osmium tetroxide (OsO_4) in a PBS buffer at pH 7.2 for 1 h, and then embedded in Epon-812 (Electron Microscopy Science). Sections 60-nm thick were aligned in single slot grids and examined under a JEOL 1010 electron microscope operated at 100 KV. Digital images were taken with a Hamamatsu camera.

Immunolocalization in sections of ovaries embedded in Lowicryl K4M

Seriated sections were treated with 10% H_2O_2 (Merck, Darmstadt, Germany) in PBS at pH 7.2 for 30 min to allow antibody-tissue interaction. After washing the slides with PBS, they were incubated with rabbit anti-tubulin (Sigma-Aldrich, St. Louis, MO, USA), rabbit anti-myosin (Sigma-Aldrich), or arabbit anti-active caspase-3 antibodies (Sigma-Aldrich) at a 1:100 dilution in PBS for 18 h at 4°C. Negative controls were made by omitting the primary antibody. Next, the slides were washed with PBS and incubated for 1 h in darkness at room temperature with secondary antibody anti-rabbit immunoglobulin coupled to FITC (Jackson Immuno-Research, West Grove, PA, USA). Sections were counterstained with DAPI 10 μg/mL (Sigma-Aldrich). Immunoassays were evaluated under a Nikon Eclipse E600 Fluorescence Microscope equipped with a Nikon Digital DXM1200F high-resolution color digital camera with a resolution of up to 12 million pixels. The objectives used were 40x and 100x. The slides were observed using DAPI (EX 330-380, BA 455-485), Texas red and Alexafluor 594 (EX 540-580, BA 600-660), and FITC filters (EX 465-495, BA 515-555). The images were recorded and processed with the Adobe Photoshop CS5 program.

Simultaneous protein immunodetection in sections of ovaries embedded in paraffin

The paraffin-embedded samples were sectioned and used to carry out immunolocalization of tubulin with LC3, Lamp-1, active caspase-3, or cytochrome C. Antigen unmasking was performed by microwaving the re-hydrated tissue sections in 0.1 M citrate-buffer at pH 6 (BioGenex, Fremont, CA, USA) in a Panasonic microwave oven for 3 min at 1,300 W, and then for 6 min at 780 W. After cooling, the sections were washed in PBS and incubated with primary antibodies for 18 h at 4°C as follows: a mixed rabbit anti-tubulin (Sigma-Aldrich) with mouse anti-cytochrome C antibodiy (Abcam, Cambridge, UK); anti-tubulin was diluted to 1:100 in PBS, and anti-cytochrome C was diluted to 1:50 in PBS. After washing, the slides were incubated for 1 h in darkness at room temperature with an anti-rabbit immunoglobulin coupled to FITC (Jackson ImmunoResearch) and anti-mouse immunoglobulin that in turn was coupled to Alexafluor 594 (Invitrogen, Carlsbad, CA, USA). Simultaneously immunodetections of tubulin with active caspase-3, LC3 or Lamp-1 were realized as follows: the sections were incubated with primary antibody , a rabbit anti-Lamp-1 (Abcam), a rabbit anti-LC3 (Thermo Scientific Pierce), or a rabbit anti-active caspase-3 (Sigma-Aldrich), all of which were diluted 1:100 in PBS. After washing the slides were incubated with Anti-Ig biotinylated Super Sensitive MultiLink (Biogenex) for 20 min. After washing the slides were incubated with anti-tubulin diluted 1:100 in PBS for 2 h at 37°C. After washing, the slides were incubated for 1 h in darkness at room temperature as follows: the anti-active caspase-3, anti-LC3, and anti-Lamp-1 were detected with Streptavidin coupled to Texas Red (Life Science Products Inc., Chestertown, MD, USA) and the tubulin was detected with an anti-rabbit immunoglobulin coupled to FITC (Jackson ImmunoResearch). Negative controls were made by omitting the primary antibodies. The preparations were then washed and counterstained with DAPI 10 μg/mL (Sigma-Aldrich) to evaluate DNA distribution. All slides were covered with mounting media

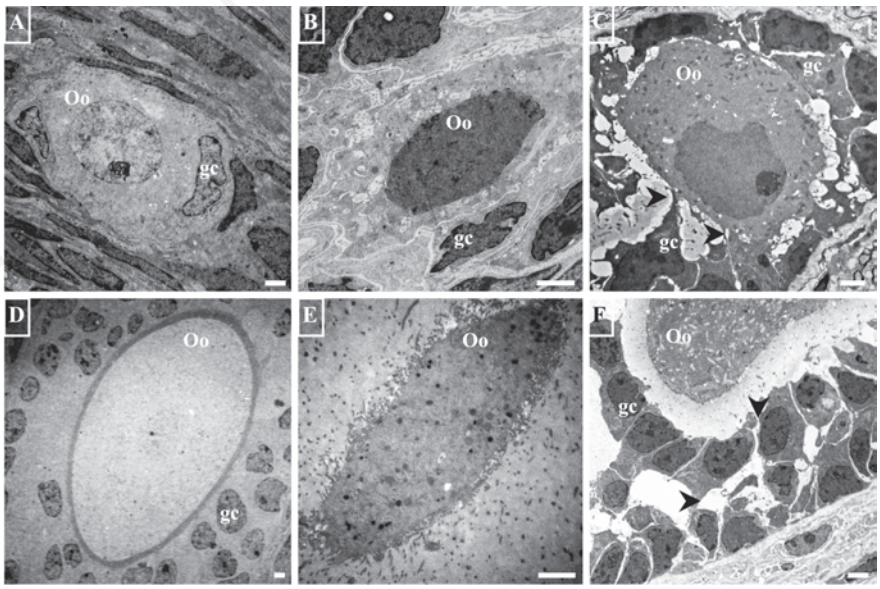

Figure 1. Electron micrographs of normal and altered oocytes of prepubertal and adult rats. A, B) Primordial follicles of prepubertal rats. A) Normal oocyte (Oo); there are no lamellae or vacuoles in its cytoplasm. B) The shape of the oocyte is altered; numerous irregularly-shaped, clear vacuoles of various sizes are present in the cytoplasm; the oocyte is in contact with only one follicular cell (gc). C) A primary follicle of prepubertal rat markedly altered in relation to highly-altered granulosa cells (gc). D) A normal secondary follicle of adult rat showing a normal relation of the oocyte with the granulosa cells (gc). E) Secondary follicle of adult rat; the oocyte has lost its relation to the granulosa cells; the pellucid zone is extremely thick. F) An antral follicle of adult rat in which granulosa cells are separated by abnormal spaces (arrow heads); the cytoplasm of the oocyte is densely vacuolated. Scale bars: 2 μm.

for fluorescence microscopy (Vectashield Mounting Medium, Vector Labs, Burlingame, CA, USA). Immunoassays were evaluated under a Nikon Eclipse E600 microscope and images were recorded with a Nikon Digital DXM1200F Camera.

Immunodetection by electron microscopy

Ultra-thin sections of Lowicryl K4M incubated with PBS for 3 min were floated in normal goat serum (NGS) diluted to 1:100 in PBS for 15 min, and incubated with primary anti-tubulin and anti-myosin antibodies diluted to 1:100 in PBS for 18 h at 4°C. They were then washed with PBS, incubated with secondary antibodies coupled to 10-nm gold micelles, rinsed with PBS, then with H_2O, and air dried. Sections were stained with uranyl acetate 0.4% for 1 min.

Western blot analyses

Oocyte isolation and culture were realized as previously reported.[4] Briefly, the ovaries were disaggregated and the cells incubated for 24 h to allow the granulosa cells to attach to the bottom of the dish. The oocytes were identified by their spherical shape and unattached localization that allowed them to be collected with a micropipette. All the oocytes obtained from two ovaries were used to the total proteins extraction. The collected oocytes were placed in lysis buffer for 15 min (50 mM Tris-Cl, pH 7.5; 150 mM NaCl, 0.1% SDS, 1 mM PMSF, 0.5% sodium deoxycholate, and 1% Nonidet P-40), supplemented with a complete protease inhibitor cocktail (Roche, Mannheim, Germany). After that, 50 µg of total proteins were loaded onto a 12% SDS-PAGE gel. Proteins were transferred to polyvinylidene fluoride membranes (PVDF), which were incubated for 1 h at room temperature in blocking buffer. Then the membranes were incubated with anti-tubulin, anti-myosin, anti-active caspase-3, anti-cytochrome C, or anti-Lamp-1 primary antibodies, at a dilution of 1:5000. Next, the proteins were tagged by incubation with peroxidase-conjugated secondary antibody (Jackson Immunoresearch, Newmarket, UK) at 1:10,000 in blocking buffer for 1 h at room temperature. Horse radish peroxidase (HRP) was used as the substrate (Immobilon Western, Millipore, CO, USA). Specific labeling was detected by chemiluminescence. The film (Hyperfilm; Amersham Biosciences, Piscataway, NJ, USA) was exposed to the membranes to detect chemiluminescence.

Results

Ultrastructural observations of atretic oocytes

Normal oocytes conserve their junctions with the granulosa cells (Figure 1 A,D), whereas oocytes that are in the process of cell death frequently have altered junctions with those cells (Figure 1 B,C). In advanced stages of the death process oocytes lose their normal shape (Figure 1 E,F) and acquire an irregular cytoplasm with numerous prolongations. The altered oocytes are present along follicular development in prepubertal (Figure 1 A-C) and adult rats (Figure 1 D-F). A frequent feature of oocytes in the cell death process is the presence of a large quantity of lamellae in the cytoplasm; however, the altered oocytes of rats younger than 14 days do not have lamellae (Figure 2A), which only appear in the oocytes of older organisms (Figure 2 B, C), and are more abundant in large, altered oocytes (Figure 2E) of prepubertal and adult rats.

Our observations allowed us to identify different arrangements of the lamellae according to the normality of the oocyte. In different

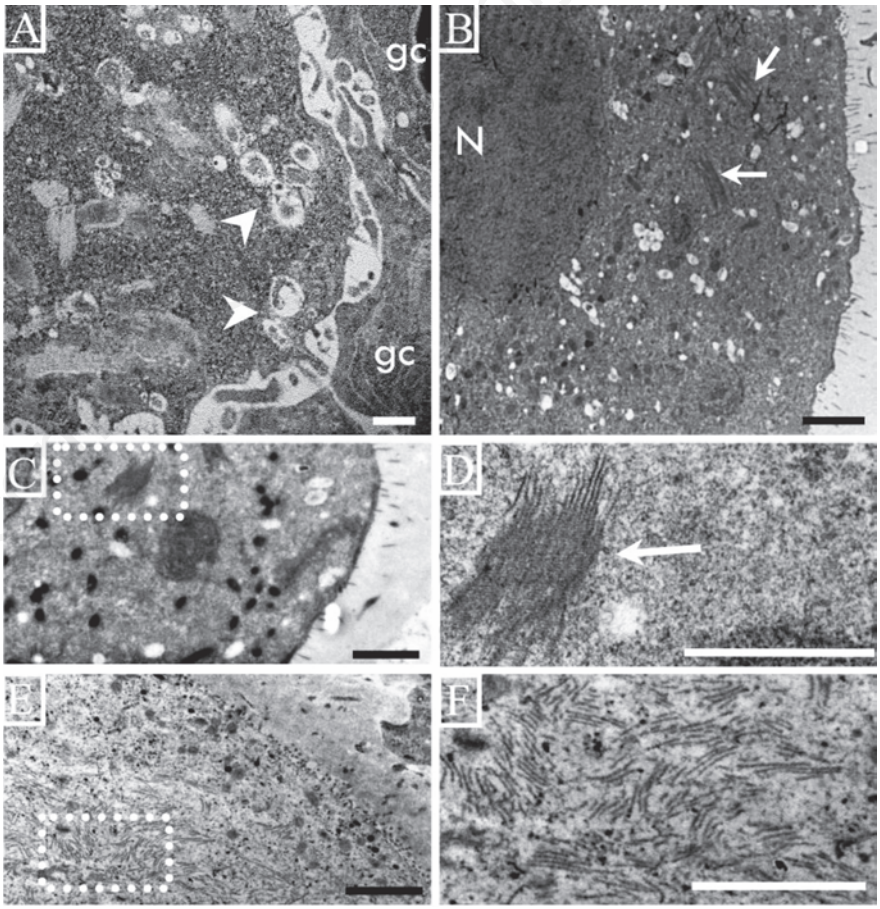

Figure 2. Electron micrographs of oocytes from rats of different ages. A) Deformed oocyte on a secondary follicle from a 13-day-old rat with numerous autophagic vesicles (arrow heads) but no lamellae in the cytoplasm; the granulosa cells (gc) are weakly-bound to the cytoplasm of the oocyte. B) An oocyte on an antral follicle from a 14-day-old rat; numerous vacuoles and groups of lamellae are present in the cytoplasm (arrows). C) Low magnification of the cytoplasm of an atretic oocyte on an antral follicle from a 15-day-old rat; there is a group of lamellae in the cytoplasm; the dotted square is enlarged in D. D) A group of lamellae forming a lattice structure. E) Numerous lamellae in the cytoplasm of an altered oocyte in an antral follicle from an adult rat; the lamellae are more abundant in the large, altered oocytes. F) High magnification of the dotted square in E showing depolymerized lamellae. Scale bars: 2 µm.

normal oocytes from antral follicles of prepubertal and adult rats, it was possible to observe a network of several lamellae that formed a lattice structure (Figure 3 A-C). In atretic oocytes the lamellas had a different arrangement, these were more abundant and their frequency changes as the process of atresia advances (Figure 3D). Oocytes in the advanced phases of destruction manifest individual lamellae (Figure 3F).

Tubulin, actin and myosin immunolocalization in plastic resin

To examine the nature of the lamellae, we immunolocalized the presence of the tubulin, myosin and actin at the light microscope level using seriated semi-thin sections, followed by ultrastructural analyses of the same areas of the same oocytes. We observed that actin is located in the periphery of the cell and that the label that identifies myosin and tubulin was dispersed in the cytoplasm (Figure 4). We also noted that the amount of fluorescence which identified the different proteins evaluated varied according to the advance of atresia in the follicle, independently of the follicular phase. In the healthy oocytes (Figure 4 A-C), label intensity was low, but in the severely-altered oocytes the amount of the label increased considerably (Figure 4D). One particularly important observation is that tubulin was the most abundant protein in the altered oocytes (Figure 4D) from follicles of prepubertal and adult rats.

The evaluation of the ultrastructure of the same area of the oocytes analyzed with the immunofluorescence to detect actin, myosin and tubulin, showed a correlation between the presence of lamellae and the intensity of tubulin labeling (Figure 5A). In healthy oocytes, tubulin labeling was low and dispersed in the cytoplasm, a finding that coincided with the low quantity of lamellae observed at the ultrastructural level (Figure 5A). Tubulin labeling in highly-altered oocytes was intense (Figure 5B) and consistent with the depolymerization and increased quantity of the lamellae observed in the ultrastructure of the oocyte (Figure 5B). The extremely low intensity of the label that evidenced actin allowed us to continue our observations while excluding this protein.

Ultrastructural distribution of the proteins myosin and tubulin

We carried out identification of the proteins tubulin and myosin in seriated sections of Lowicryl by permitting their ultrastructural immunolocalization and correlation with light microscope observations. Once we identified the same areas under both light and electron microscopy, they were photographed. This allowed us to determine that the zones which

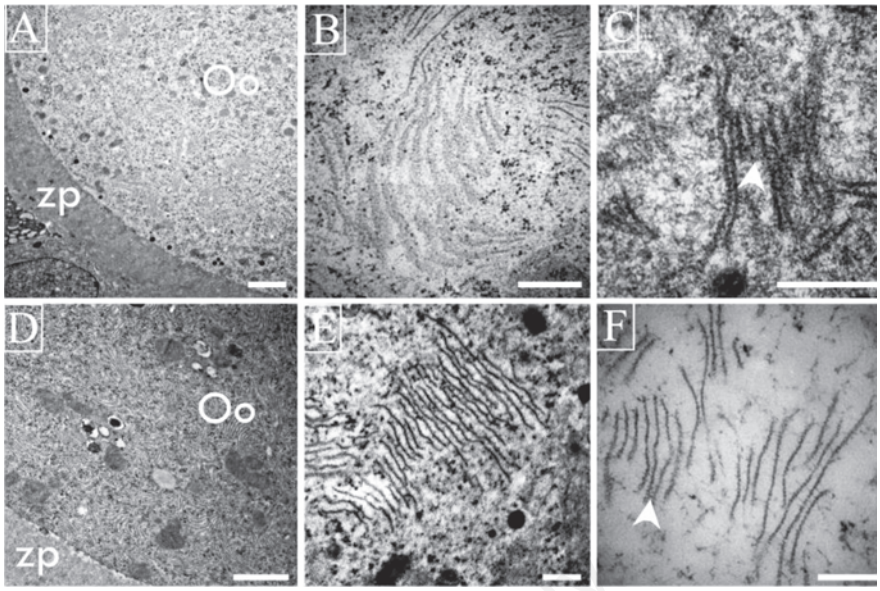

Figure 3. Ultrastructural views of lamellae in different oocytes from antral follicles of adult rats. A-C) Lamellae in healthy oocytes form lattices; in C one can observe the strong relation among the several lamellae units that form lattices (arrow head). D-F) Altered oocyte shows depolymerized lamellae present as fibrous units visible under high magnification (F) of zones of the same oocytes illustrated in D (arrow head). Scale bars: A,D) 2 µm; remaining panels: 200 nm.

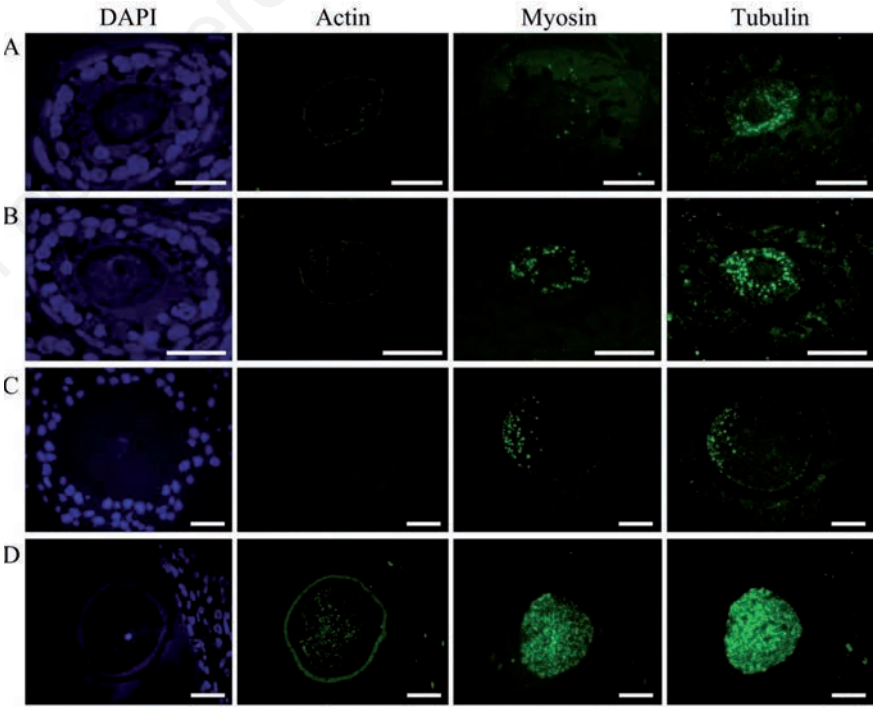

Figure 4. Immunodetection of the proteins actin, myosin and tubulin in semi-thin sections. A,B) Secondary follicles. C,D) Antral follicles of adult rats. DAPI shows DNA distribution in nuclei from granulosa cells and oocytes. Actin distribution is confined to the periphery of the oocyte and scarce in the cytoplasm. Myosin and tubulin are dispersed in the cytoplasm. Tubulin is more abundant than myosin. The amount of myosin and tubulin is significantly higher than in the non-altered oocyte (A, B, C). The images in D illustrate a highly-altered oocyte. Scale bars: 20 nm.

were highly-positive to tubulin and myosin immunolocalization corresponded to areas with the highest density of positive lamellae observed at the ultrastructural level. Moreover, in those areas the lamellae showed an intense presence of tubulin (Figure 6). The significant correspondence between areas with high lamellae density and intense tubulin labeling allowed us to continue our study by evaluating only the relationship between the type of cell death and tubulin distribution.

Immunodetection of tubulin and cell death proteins

In order to identify the type of cell death that took place in the oocytes, and the changes in the patterns of tubulin distribution, we identified pro-apoptotic and pro-autophagic proteins and tubulin in the same cells (Figure 7). Observations indicate that the presence of the pro-apoptotic active caspase-3 protein coincided with a regionalized, elevated labeling of anti-tubulin in the oocytes (Figure 7B) and the depolymerized lamellae (Figure 7B, bottom). In the oocytes that tested negative for the caspases, tubulin was distributed in the cytoplasm (Figure 7A), and the lamellae formed lattices (Figure 7B, bottom). The polymerized and depolymerized lamellae were ultrastructurally positive to the tubulin protein (Figure 7, bottom). Subsequently, simultaneous cytochrome-C and tubulin protein as well as active caspase-3 and tubulin protein immunodetection in paraffin embedded sectioned ovaries, showed that in the non-altered oocytes from antral follicles of adult rats the tubulin is dispersed through the cytoplasm (Figure 8). However, the apoptotic oocytes with a high level of cytochrome-C and active caspase-3 proteins have tubulin distributed in cumuli (Figure 8). To further test apoptosis-induced lamellae depolymerization, immunodetection to identify pro-autophagic cell death proteins was conducted simultaneously. Results indicate that the oocytes that were highly positive to the Lamp-1 and LC3 proteins had a homogeneous distribution of the tubulin (Figure 8).

To corroborate the association of autophagy with tubulin and/or lamellae the ultrastructural presence of vesicles was evaluated. Our observations indicate that, in fact, the oocytes with a high amount of autophagic vesicles presented low quantities of depolymerized lamellae (Figure 9).

Western blot protein analyses

Expression of the proteins evaluated during these experiments was identified by the electrophoresis of proteins obtained from isolated oocytes. The results evidenced the expression of the pro-autophagic proteins Lamp-1 and LC3 (LC3-I and LC3-II) in the cellular extracts. The pro-apoptotic proteins cytochrome-C and active caspase-3 were also present in the samples evaluated. The proteins tubulin and myosin were evident in the oocytes; indeed, tubulin was present in three different isoforms (Figure 10A). Negative controls to the immunodetections realized are shown in Figure 10B.

Discussion

The ultrastructure of oocytes has been studied for several years. Vázquez-Nin and Sotelo[14] identified the presence of cytoplasmic lamellae during the process of atresia in mammal oocytes. Today, these lamellae are known as cytoplasmic lattices, or simply lattices and some of their molecular and functional characteristics have been identified.[16,17] Our observations demonstrate the presence of lamellae in stacks in healthy oocytes, whose ultrastructural characteristics evidence a non-altered follicle. However, in the follicles with altered shapes and detached granulosa cells the lamellae have arrangements of individual filaments dispersed in the cytoplasm of the oocytes. In normal oocytes, these lattices have been considered as sites of RNA storage,[16,18] which are deemed important for the first phases of development after the fertilization event.[18] We consider that the altered arrangement of the lamellae could to contribute to incorrect RNA storage in the oocytes that are destined for elimination, and that this could be related to the different

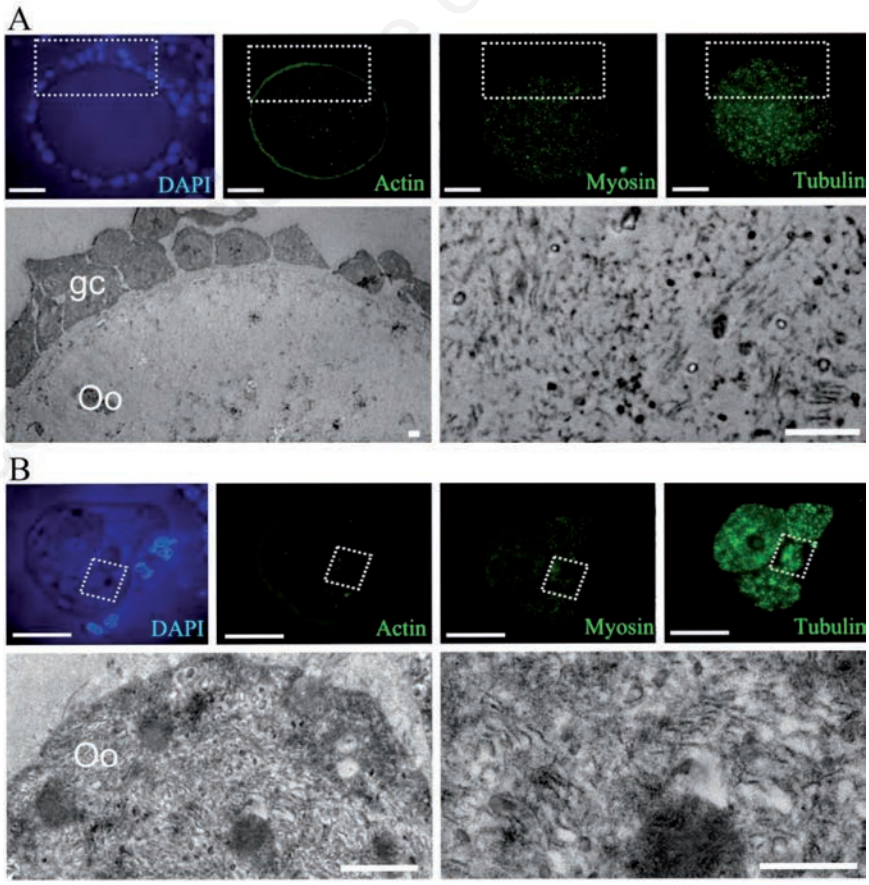

Figure 5. Optical immunodetection of the proteins actin, myosin and tubulin in a normal oocyte (A), and an altered oocyte (B), with ultrastructural evaluation on antral follicles. A) The normal oocyte displays a peripheral pattern of actin distribution, while myosin and tubulin are distributed in the cytoplasmic space; the electron microscopy image shows the square area illustrated in the semi-thin sections, evidencing the small amount of lamellae that corresponds to the low quantity of immunolabeling. B) A highly-altered, segmented oocyte with a high amount of tubulin; the ultrastructure of the squared zone is shown in the lower panel, evidencing a high amount of depolymerized lamellae. Scale bars: optical images, 20 µm; electron microscopy images, 2 µm.

pathways of cell death. The fact that lamellae are observed in the oocytes of those organisms at peri-ovulatory age suggests that these structures are related to the maturity and quality of the germinal cells, because they are absent in infant and juvenile individuals (*i.e.*, days 1-14 post-birth) that are far from reaching puberty and first ovulation. We found that the lattices begin to form when the oocytes reach the initial phase of antral formation; that is, from day 14 post-birth.

Our observations of the presence of the protein tubulin and its close relation to the lamellae support the idea that these structures –the lamellae– are elements of the cytoskeleton. Microtubules are formed by the polymerization of tubulin monomers, which are major cytoskeletal elements found in mammalian oocytes that play a crucial role in meiotic/mitotic events.[19] Inside the ovary, oocytes are arrested in the prophase of the first meiotic division when the microtubules are long, stable and radiate throughout the cytoplasm,[20] as we observed in the structurally-normal oocytes. Similarly, we found that there is a relation between the increased depolymerization of the lamellae and the advance of oocyte alteration. Moreover, the amount of individual lamellae correlated with the highly-dense, fragmented oocytes, which were enriched in tubulin and myosin, as well as with the depolymerized lamellae.

The different distribution patterns of the protein tubulin in the oocytes are related to morphological alterations. In normal oocytes, tubulin is distributed homogeneously, while in altered ones we identified a patchwork distribution pattern that suggests protein disarrangement. Ultrastructural observation of those same sections allowed us to identify the loss of integrity of the lattices, suggesting a correlation between the disassembled lamellae and the altered pattern of tubulin distribution. The staining pattern of tubulin changed visibly as the atresia process advanced. The initial oocyte degradation process is characterized by the lower quantity of labeled tubulin at the light and ultrastructural levels. The simultaneous optical and ultrastructural evaluation of the immunodetection of tubulin and myosin in seriated slides strengthens our affirmation that the nature of the lamellae corresponds to elements of the cytoskeleton.

Considering that oocytes are eliminated during the atresia process by different types of programmed cell death,[3,4] we evaluated the behavior of the different patterns of altered lamellae during apoptotic and autophagic cell death and ascertained that pro-apoptotic proteins such as active caspase-3 and cytochrome-c were present in those oocytes that had an altered pattern of tubulin distribution. In contrast, in the oocytes with increased labeling of the Lamp-1 and LC3 proteins (which identified the autophagic process) tubulin distribution, was not altered. In this regard, we know that the caspases have a series of substrates that are involved in maintaining the cytoskeletal architecture, and that their cleavage is directly related to apoptotic changes in cell shape (reviewed in [21]). We observed that the highly-compacted, fragmented oocytes with intense labeling of active caspase-3 possess an increased amount of depolymerized lamellae and this allowed us to affirm that caspase-3 participation during the apoptosis process alters the structure of the lamellae. In this regard, we know that the morphological changes suffered by the cells during apoptosis are a consequence of the enzymatic processes triggered by caspase activation. The role of the microtubules during apoptosis is interesting because at first they suffer depolymerization, but in the late phases they are involved in the correct formation of apoptotic bodies[22] and the preservation of plasmatic membrane integrity.[23] Thus, we can hypothesize that proteolysis of the substrates of the caspases probably leads to the destructive alterations observed in atretic oocytes, such as the depolymerization of lamellae. Moreover, the well-known ability of active caspase-3 to cleave cytoskeleton proteins[24,25] allows us to suggest that the modulation of the lamellar structure could be affected by the presence of the protease in its active form, as shown in the present study. On the other hand, we were also able to discern that in the oocytes that were positive to autophagic proteins, tubulin was distributed in the cytoplasmic volume. During the autophagic process, LC-3 protein (mammalian microtubule-associated protein

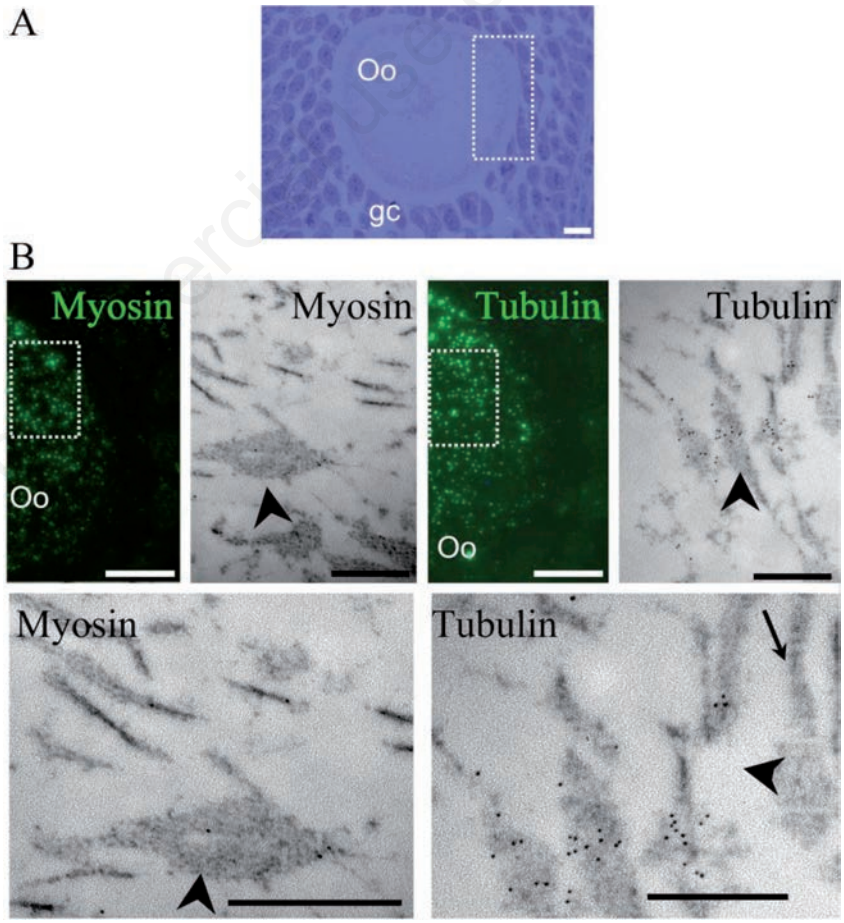

Figure 6. Light microscopy and ultrastructural immunolocalization of the proteins myosin and tubulin on oocytes from antral follicle. A) Semi-thin sections stained with toluidine blue show the morphological characteristics of the evaluated oocyte (Oo) surrounded by granulosa cells (gc). B) Immunodetection of the proteins myosin and tubulin in continuous sections; tubulin was more abundant than myosin; the dotted square area was evaluated at the ultrastructural level and the same proteins were identified, evidencing the presence of a low amount of myosin and an increased level of tubulin. Scale bars: light microscopy images, 10 µm; electron microscopy images, 500 nm.

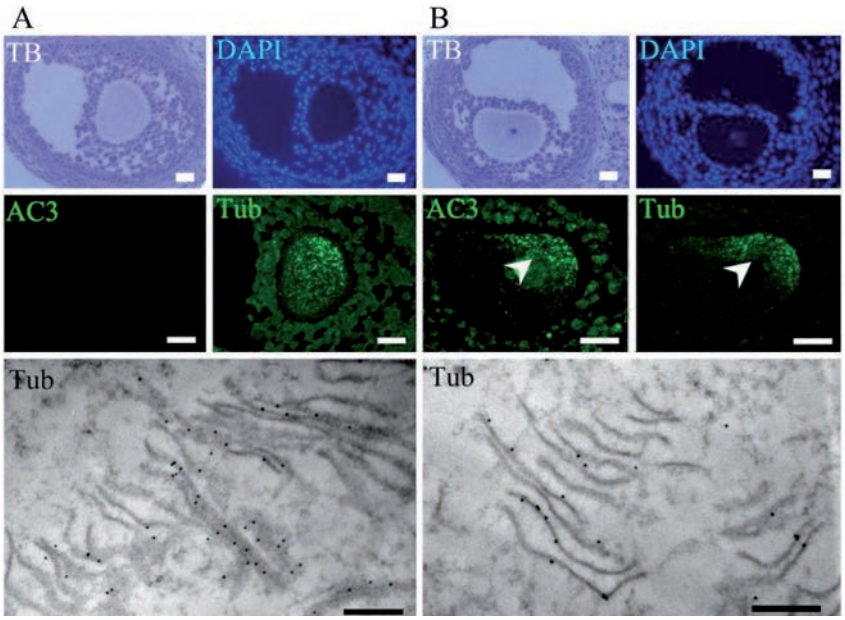

Figure 7. Immunodetection of active caspase-3 and tubulin on oocytes from antral follicles. A) Normal oocyte with cytoplasm that is negative to active caspase-3 (AC3); the toluidine blue stain (TB) shows the general morphology of the altered follicle; the tubulin (Tub) label is distributed in the cytoplasm; at the ultrastructural level, lattice-like structures were observed with a high quantity of tubulin labeling (lower panel). B) Altered oocyte positive to active caspase-3; the tubulin is regionalized to form cumuli; at the ultrastructural level, several depolymerized lamellae were observed in the same region, which were positive for tubulin immunodetection (lower panel). Scale bars: light microscopy images, 20 µm; electron microscopy images, 500 nm.

1 light chain 3) lipidation is a necessary process to initiate autophagic vesicle formation. Its interaction with other proteins, such as MAP1A or 1B, modulates the shape of the microtubules.[26] The fact that depolymerized lamellae were more abundant in the apoptotic oocytes than the autophagic ones, can thus be related to the role of these proteins in the autophagy process.

All these results provide information regarding the different changes in the dynamics of cytoskeleton components during the atresia process in ovaries. This research indicates the presence of apoptotic and autophagic cell death in the oocytes, and their relation to modifications of the microtubules/lamellae. Cellular morphology is modulated by the cytoskeleton, and during cell death events several morphological changes occur that involve remodeling of the cytoskeleton. During apoptosis we observed the break-up of the microtubules *via* caspase activity, while during autophagy several proteins are related to the dynamics of the cytoskeleton. These processes produce the different patterns that the lamellae/tubulin acquire during apoptotic and autophagic cell death. The connection between the advance of cell death and the depolymerization of lamellae was initiated more by the pro-apop-

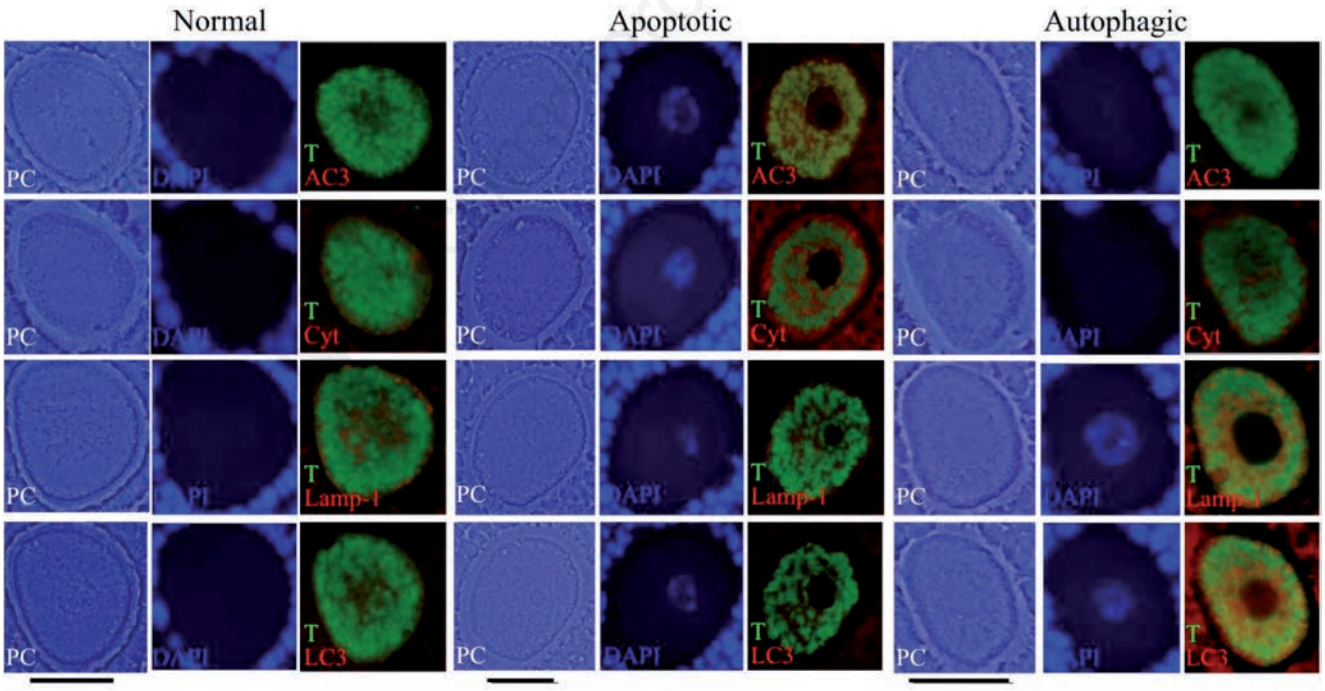

Figure 8. Simultaneous light immunolocalization of tubulin with apoptotic and autophagic proteins, in continuous sections of paraffin-embedded samples on oocytes from antral follicles. Phase contrast illumination (PC) evidences the different morphology corresponding to normal and altered oocytes (apoptotic and autophagic). In the normal oocyte the green label shows tubulin (T) distributed homogenously in the cytoplasmic space that coincides with a basal label to cytochrome-C (Cyt), Lamp-1 and LC3 proteins as well as the negative label to active caspase-3 (AC3). In the apoptotic oocyte the aggregated tubulin distribution coincides with an increased label to cytochrome-C and the positive reaction to the active caspase-3. In the autophagic oocyte the tubulin is distributed homogenously in the cytoplasmic space and does not form aggregates. This oocyte has an increased level of Lamp-1 and LC3 proteins. DAPI is evidencing the chromatin distribution in the nuclear space. Scale bars: 30 µm.

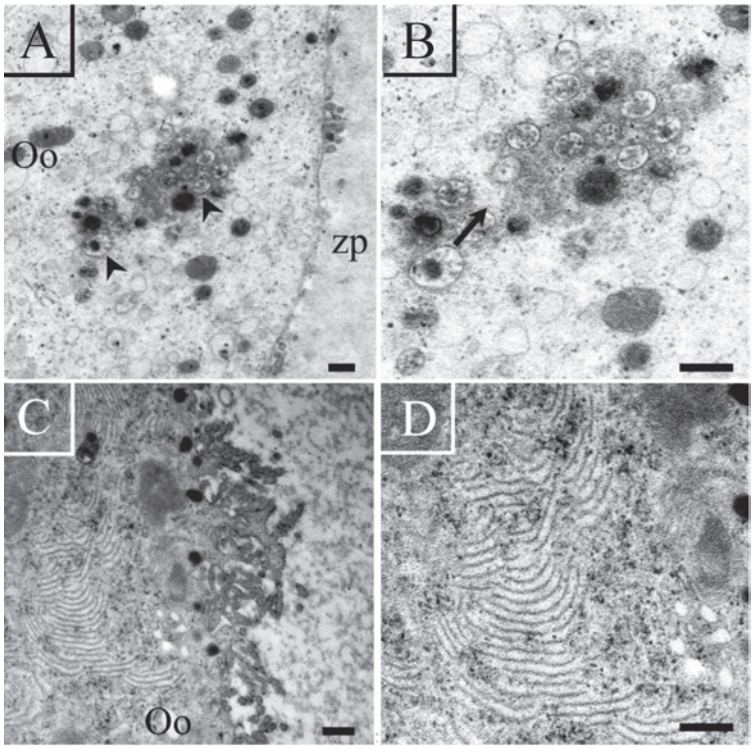

Figure 9. Ultrastructural visualization of altered oocytes from antral follicles. A) Autophagic vesicles (arrow) are present in the cytoplasm of the oocyte (Oo); some cytoplasmic prolongations of the granulosa cells are observed (arrow heads). B) High magnification of the same oocyte observed in A; the autophagic vacuoles are indicated by an arrow; the oocyte has no lamellae. C) Region of a fragmented oocyte with a high quantity of lamellae. D) High magnification of the same oocyte shown in C; the presence of depolymerized lamellae is observed in its cytoplasm. Scale bars: left panels, 2 µm; right panels, 500 nm.

totic than by the pro-autophagic proteins, as evidenced by the fact that the oocytes eventually manifested a collapsed shape.

References

1. Ortiz R, Echeverría OM, Salgado R, Escobar ML, Vázquez-Nin GH. Fine structural and cytochemical analysis of the processes of cell death of oocytes in atretic follicles in new born and prepubertal rats. Apoptosis 2006;11:25-37.
2. Escobar ML, Echeverría OM, Casasa AS, García G, Aguilar SJ, Vázquez-Nin GH. Involvement of pro-apoptotic and pro-autophagic proteins in granulosa cell death. Cell Biology 2013;1:9-17.
3. Escobar ML, Echeverría OM, Ortiz R, Vázquez-Nin GH. Combined apoptosis and autophagy, the process that eliminates the oocyte of atretic follicles in immature rats. Apoptosis 2008;13:1253-66.
4. Escobar ML, Echeverría OM, Sánchez-Sánchez L, Méndez C, Pedernera E, Vázquez-Nin GH. Analysis of different cell death processes of prepubertal rat oocytes in vitro. Apoptosis 2010;15:511-26.
5. Escobar ML, Echeverría OM, Vázquez-Nin GH. Immunohistochemical and ultrastructural visualization of different routes of oocyte elimination in adult rats. Eur J Histochem 2012;56:e17.

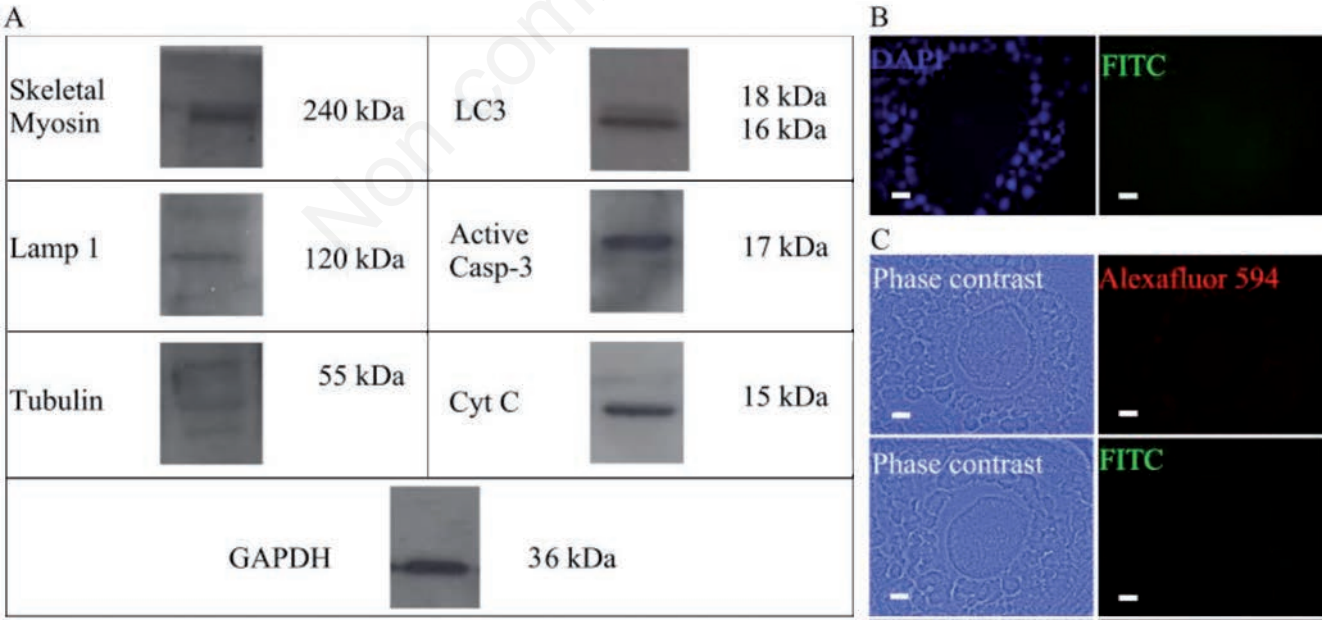

Figure 10. Western blot analysis and negative controls for the different light immunolocalizations performed. A) Analyses of total myosin, Lamp 1, tubulin, (LC3-I and LC3-II), active caspase-3, and cytochrome-C from isolated oocytes; the presence of the different proteins evaluated was evidenced in the Western Blot assays using total proteins from isolated oocytes. B) Negative control to the immunodetection realized in semi-thin sections. C) Negative control to the immunodetection realized in sectioned paraffin-embedded samples. Scale bars: 10 µm.

6. Kerr JF, Wyllie AH, Currie AB. Apoptosis. A basic biological phenomenon with wide-ranging implications in tissue kinetics. Br J Cancer 1972;26:239-57.
7. Thornberry NA, Lazebnik Y. Caspases: enemies within. Science 1998;281:1321-6.
8. Baud V, Karin M. Signal transduction by tumor necrosis factor and its relatives. Trends Cell Biol 2001;11:372-7.
9. Chen YR, Kori R, John B, Tan TH. Caspase-mediated cleavage of actin- binding and SH3-domain-containing proteins, cortactin, HS1, and HIP-55 during apoptosis. Biochem Biophys Res Commun 2001;288:981-9.
10. Kook S, Kim DH, Shim SR, Kim W, Chun JS, Song WK. Caspase-dependent cleavage of tensin induces disruption of actin cytoskeleton during apoptosis. Biochem Biophys Res Commun 2003;303:37-45.
11. Eskelinen EL, Saftig P. Autophagy: a lysosomal degradation pathway with a central role in health and disease. Biochim Biophys Acta 2009;1793:664-73.
12. Yang Z, Klionsky DJ. Mammalian autophagy: core molecular machinery and signaling regulation. Curr Opin Cell Biol 2010;22:124-31.
13. Kabeya Y, Mizushima N, Ueno T, Yamamoto A, Kirisako T, Noda T, et al. LC3, a mammalian homologue of yeast Apg8p, is localized in autophagosome membranes after processing. EMBO J 2000;19:5720-8.
14. Vázquez-Nin GH, Sotelo JR .Electron microscope study of the atretic oocytes of the rat. Z Zellforsch Mikrosk Anat 1967;80:518-33.
15. National Research Council. Guidelines for the care and use of laboratory animals. National Academies Press, Washington, DC, USA; 1996.
16. Yurttas P, Vitale PM, Fitzhenry RJ, Cohen-Gould L, Wu W, Gossen JA, et al. Role for PADI6 and the cytoplasmic lattices in ribosomal storage in oocytes and translational control in the early mouse embryo. Development 2008;135:2627-36.
17. Kan R, Yurttas P, Kim B, Jin M, Wo L, Lee B, et al. Regulation of mouse oocyte microtubule and organelle dynamics by PADI6 and the cytoplasmic lattices. Dev Biol 2011;350:311-22.
18. García RB, Pereyra-Alfonso S, Sotelo R. Protein-synthesizing machinery in the growing oocyte of the cyclic mouse. A quantitative electron microscopic study. Differ 1979;14:101-6.
19. Kwon DJ, Lee YM, Hwang IS, Park CK, Yang BK, Cheong HT. Microtubule distribution in somatic cell nuclear transfer bovine embryos following control of nuclear remodeling type. J Vet Sci 2010; 11:93-101.
20. Albertini DF. Regulation of meiotic maturation in the mammalian oocyte: interplay between exogenous cues and the microtubule cytoskeleton. Bioessays 1992;14:97-103.
21. Fischer U, Jänicke RU, Schulze-Osthoff K. Many cuts to ruin: a comprehensive update of caspase substrates. Cell Death Differ 2003; 10:76-100.
22. Lane JD, Allan VJ, Woodman PG. Active relocation of chromatin and endoplasmic reticulum into blebs in late apoptotic cells. J Cell Sci 2005;118(Pt 17):4059-71.
23. Sánchez-Alcázar JA, Rodríguez-Hernández A, Cordero MD, Fernández-Ayala DJ, Brea-Calvo G, Garcia K, et al. The apoptotic microtubule network preserves plasma membrane integrity during the execution phase of apoptosis. Apoptosis 2007;12: 1195-208.
24. Gerner C, Frohwein U, Gotzmann J, Bayer E, Gelbmann D, Bursch W, et al. The Fas-induced apoptosis analyzed by high throughput proteome analysis. J Biol Chem 2000;275:39018-26.
25. Adrain C, Duriez PJ, Brumatti G, Delivani P, Martin SJ. The cytotoxic lymphocyte protease, granzyme B, targets the cytoskeleton and perturbs microtubule polymerization dynamics. J Biol Chem 2006;281:8118-25.
26. Mann SS, Hammarback JA. Molecular characterization of light chain 3. A microtubule binding subunit of MAP1A and MAP1B. J Biol Chem 1994;269:11492-7.